Molecules and Cells

Sertad1 Induces Neurological Injury after Ischemic Stroke via the CDK4/p-Rb Pathway

Jianxiong Li[1], Bin Li[1], Yujie Bu[1], Hailin Zhang[2,*], Jia Guo[1], Jianping Hu[1], and Yanfang Zhang[1]

[1]Department of Neurology, Lanzhou University Second Hospital, Lanzhou 730030, China, [2]Neurosurgery, Lanzhou University Second Hospital, Lanzhou 730030, China
*Correspondence: ldyy_zhanghlzhl@lzu.edu.cn
https://doi.org/10.14348/molcells.2021.0071
www.molcells.org

SERTA domain-containing protein 1 (Sertad1) is upregulated in the models of DNA damage and Alzheimer's disease, contributing to neuronal death. However, the role and mechanism of Sertad1 in ischemic/hypoxic neurological injury remain unclear. In the present study, our results showed that the expression of Sertad1 was upregulated in a mouse middle cerebral artery occlusion and reperfusion model and in HT22 cells after oxygen-glucose deprivation/reoxygenation (OGD/R). Sertad1 knockdown significantly ameliorated ischemia-induced brain infarct volume, neurological deficits and neuronal apoptosis. In addition, it significantly ameliorated the OGD/R-induced inhibition of cell viability and apoptotic cell death in HT22 cells. Sertad1 knockdown significantly inhibited the ischemic/hypoxic-induced expression of p-Rb, B-Myb, and Bim *in vivo* and *in vitro*. However, Sertad1 overexpression significantly exacerbated the OGD/R-induced inhibition of cell viability and apoptotic cell death and p-Rb, B-Myb, and Bim expression in HT22 cells. In further studies, we demonstrated that Sertad1 directly binds to CDK4 and the CDK4 inhibitor ON123300 restores the effects of Sertad1 overexpression on OGD/R-induced apoptotic cell death and p-Rb, B-Myb, and Bim expression in HT22 cells. These results suggested that Sertad1 contributed to ischemic/hypoxic neurological injury by activating the CDK4/p-Rb pathway.

Keywords: CDK4, neurological injury, oxygen-glucose deprivation/reoxygenation, p-Rb, Sertad1

INTRODUCTION

Cerebral ischemia accounts for 87% of all stroke cases and is one of the leading causes of death and disability globally (Kuriakose and Xiao, 2020; Russo et al., 2011). Ischemic stroke due to lack of oxygen, glucose, and other nutrients alters intracellular metabolism, ultimately resulting in neuronal death (Auriel and Bornstein, 2010), which is the most prominent pathological change in cerebral ischemia and causes the irreversible loss of brain function (Wei et al., 2016). Thus, neuroprotective strategies can be used in maintaining adequate brain and neuronal functions after ischemia and reperfusion injury. However, thrombolysis with a tissue plasminogen activator is the only U.S. Food and Drug Administration-approved neuroprotective treatment that has a narrow therapeutic window (3-4.5 h after symptom onset) (Hacke et al., 2008). Other ischemic neuroprotective treatments, such as calcium channel blockers, N-methyl-D-aspartate (NMDA) receptor antagonists, and antioxidants, cannot reverse neuronal damage following ischemia and reperfusion injury (Adams, 2001). Therefore, the precise mechanisms underlying neuronal injury after cerebral ischemia should be investigated to identify new targets for neuroprotection.

SERTA domain-containing protein 1 (Sertad1), also known as transcriptional regulator interacting with PHD-bromodomain 1 (Trip-Br1) or p34 (SEI-1), is a member of the Sertad family (Lai et al., 2007) and functions as an oncoprotein in many tumors (Hu et al., 2019; Li et al., 2016; You et al.,

Received 25 March, 2021; revised 19 November, 2021; accepted 9 December, 2021; published online 3 January, 2022

eISSN: 0219-1032

2017). For example, Li et al. (2016) showed that Sertad1 inhibition accelerates hypoxia-induced cell apoptosis in breast cancer cell lines. Hu et al. (2019) suggested that Sertad1 promotes the proliferation of prostate cancer cells and thereby contributes to prostate cancer progression. Sertad1 acts as a growth factor sensor and facilitates the formation and activation of cyclin D/CDK4 complexes (Sugimoto et al., 1999). Cyclin D/CDK4/pRb activation contributes to neuronal death induced by thrombin, DNA damage, nerve growth factor (NGF) withdrawal or ischemic insult (Iyirhiaro et al., 2017; Liu and Greene, 2001; Rao et al., 2007; Rashidian et al., 2005). Moreover, Biswas et al. (2010) found that Sertad1 is essential to neuronal death induced by NGF withdrawal and β-amyloid in the cerebral cortex. Therefore, in the present study, we hypothesized that Sertad1 plays an important role in ischemic/hypoxic neurological injury and investigated its role and molecular mechanisms in ischemic/hypoxic neurological injury.

MATERIALS AND METHODS

Experimental animals

C57BL/6 male mice aged 6 to 8 weeks were obtained from Lanzhou University Second Hospital. All the mice were subjected to 12 h light/12 h dark cycle and had free access to water and food. Animal experiments were conducted in accordance with the guidelines of the Institutional Animal Care and Use Committee of the Institute of Nutrition and Health. All animal procedures were approved by the Ethics Committee of Lanzhou University Second Hospital (No. D2020-46).

Middle cerebral artery occlusion and reperfusion (MCAO/R) model

Mouse focal brain ischemia was induced by MCAO/R in male C57BL/6J mice with the intraluminal filament method as described previously (Kuo et al., 2016; Liu et al., 2012). Briefly, the mice were anesthetized with ketamine (12 mg/kg) and xylazine (10 mg/kg), fixed on an operating table in the supine position, and maintained at 37.0°C ± 0.5°C during surgery. The right carotid bifurcation was next exposed through a midline neck incision. A silicone-coated 8-0 filament was inserted through the common carotid artery and advanced (9.0-10.0 mm) gently for the occlusion of the middle cerebral artery. The regional cerebral blood flow during surgery was detected to confirm the successful occlusion by laser Doppler flowmetry (PerifluxSystem 5000; Perimed, Sweden). After 1 h of occlusion, the nylon suture was removed for the restoration of cerebral blood flow. In the sham group, the common carotid arteries were surgically exposed without subsequent MCAO.

Neurobehavioral evaluation

Neurobehavioral evaluation was performed 48 h after reperfusion in accordance with a previously described method (Longa et al., 1989; Zhang et al., 2018). Briefly, neurobehavioral evaluation was scored using a five-point scale: 0, no neurological deficit; 1, failure to extend left forepaw fully; 2, circling to the left; 3, inability to bear weight on the left; 4, no spontaneous walking with depressed level of consciousness.

Infarct volume assessment

Infarct volume assessment was performed 48 h after reperfusion and determined by 2,3,5-triphenyltetrazolium chloride (TTC) staining. Briefly, the mice were euthanized under anesthesia, and their brains were rapidly removed and cut into 2-mm-thick slices. TTC solution (2%; Solarbio, China) was used to stain the slices at 37°C for 30 min. The infarction volume was measured using Image J software (National Institutes of Health, USA).

Immunofluorescence staining

Mice were anesthetized 48 h after reperfusion, transcardially perfused with phosphate-buffered saline (PBS), and fixed with 4% paraformaldehyde. Their brains were rapidly removed and postfixed with 4% paraformaldehyde. Brains were then immersed in 20% and 30% sucrose overnight at 4°C, embedded in Tissue-Tek OCT compound (Sakura, Japan), and subjected to section on a freezing microtome. The sections (10 μm) were washed with PBS and blocked in QuickBlock™ immunostaining blocking solution (Beyotime, China) for 1 h at room temperature and incubated overnight at 4°C with the following primary antibodies: rabbit anti-Sertad1 (1:200, ARP34309_T100; AVIVA, USA), mouse anti-NeuN (1:100, 66836-1-Ig; Proteintech, China), mouse anti-GFAP (1:200, ab279290; Abcam, USA), mouse anti-Iba1 (1:500, GT10312; GeneTex, USA). After washing, the sections were incubated with Alexa Fluor Plus 488 goat anti-rabbit secondary antibody (1:200, A32731; Thermo Fisher Scientific, USA) or Alexa Fluor Plus 555 goat anti-mouse secondary antibody (1:200, A32727; Thermo Fisher Scientific) at 37°C for 1 h. DAPI (Beyotime) was used to stain cellular nuclei at 37°C for 10 min. Finally, the sections were photographed using a microscope with a digital camera (Olympus, Japan).

Stereotactic surgery

Adeno-associated virus (AAV) 9-Syn-GFP-U6-shSertad1 (AAV-shSertad1) and AAV9-Syn-GFP-U6-negative control (AAV-shCon) were obtained from Sunbio Medical Biotechnology (China). The sequences of shSertad1 and shCon used in this study were as follows: shSertad1: 5′- CCGGGAATTGACTTGGATCTGAGTTCTCGAGTTCTCAGATCCAAGTCAATTC-3′; shCon: CCGGTTCTCCGAACGTGTCACGTCTCGAGACGTGACACGTTCGGAGAA-3′. A total of 5×10^9 genome copies of AAV-shSertad1 or AAV-shCon virus in 3 μl were stereotactically injected into the right lateral ventricle (bregma: −2.2 mm, dorsoventral: 3 mm, lateral: 1 mm) at a rate of 200 nl/min (Jin et al., 2019; Wu et al., 2017). After injection, the needle was maintained for 10 min prior to withdrawal.

Cell culture and oxygen-glucose deprivation/re-oxygenation (OGD/R) model

The HT22 cells were obtained from Procell Life Science & Technology (China; CL-0595) and cultured in DMEM with 10% FBS at 37°C. To induce OGD, the neurons were cultured in glucose-free DMEM solution and maintained in a hypoxic chamber (Thermo Fisher Scientific) at 94% N_2, 1% O_2, 5% CO_2 and 37°C for 2, 4, 8, or 12 h, as previously described (Chen et al., 2011; Xu et al., 2018). The HT22 cells in the normal group were subjected to OGD for 0 h. After OGD,

the neurons were cultured in a normal DMEM solution with 10% FBS for 24 h or 48 h. After 24 h or 48 h of re-oxygenation, neurons were subjected to later assay.

Cell transfection

To knockdown Sertad1 expression in the HT22 cells, the scramble control siRNA (siCon) and Sertad1 siRNA (siSertad1) were designed and synthesized by GenePharma (China). The siRNA sequences were as follows: siSertad1: 5′-GAAUUGACUUGGAUCUGAGUUTT-3′; siCon: 5'-UUCUCCGAACGUGUCACGUTT-3′. To upregulate Sertad1 expression in HT22 cells, the pcDNA3.1 negative control plasmid (pcDNA3.1) and the Sertad1-3flag expression plasmid (Sertad1 ov) were purchased from Sunbio Medical Biotechnology. Two days before OGD/R, a total of 5×10^5 HT22 cells were plated in six-well plates and transfected using Lipofectamine® 2000 Reagent (Thermo Fisher Scientific) in accordance with the manufacturer's instructions.

Cell viability assay

For the cell viability assay, HT22 cells were transfected for 48 h, seeded at a density of 1×10^4 cells/well on 96-well plates for 24 h, and then subjected to OGD/R. The medium was then removed and 10 μl of Cell Counting Kit-8 (CCK-8) solution (Beyotime) was added to each well. After incubation for 1 h at 37°C, the absorbance was measured using an automatic microplate reader (Bio-Tek M200; Tecan, Austria) at 450 nm. Cell viability was assessed as the percentage of viable cells relative to the vehicle groups.

TUNEL assay

Cell apoptosis in the ischemic penumbra was detected using TUNEL assay (Roche Diagnostics, USA) in accordance with the manufacturer's instructions. Briefly, dead cells were stained with TUNEL solution (red), and the neurons were stained with NeuN antibody (blue). The collocation of red (TUNEL) and blue (NeuN) indicated the dead neurons. The percentages of TUNEL-positive neurons relative to the NeuN-positive cells were regarded as the death index. The sections were photographed using a microscope with a digital camera (Olympus). Five different fields (×200 magnification) per section were selected, and the number of TUNEL positive neurons and the number of neurons were then counted (Liu et al., 2020). The percentage of TUNEL positive neurons per mouse was obtained from three sections. Six mice per group were analyzed. The image analysis was performed blindly.

To determine the cell death after OGD/R, a TUNEL assay was performed in accordance with the manufacturer's protocol. Briefly, HT22 cells were transfected for 48 h, seeded at a density of 1×10^5 cells/well on 24-well plates on glass coverslips for 24 h, and subjected to OGD/R. After OGD/R, the medium was removed. Next, the cells were fixed in 4% paraformaldehyde for 30 min and incubated in 0.3% Triton X-100 for 5 min. TUNEL solution (50 μl) was added to each well for 1 h at 37°C. After washing with PBS, cell nuclei were stained with DAPI. TUNEL-positive cells were counted from three fields under a fluorescence microscope at 200× magnification. The percentages of apoptotic cells were assessed by averaging the TUNEL-positive cells relative to the DAPI-positive cells across the three fields (Wang et al., 2013).

Real-time quantitative polymerase chain reaction (RT-qPCR)

After treatment, brain tissues and HT22 cells were collected. Total RNA was isolated using TRIzol reagent (Invitrogen, USA), and cDNA was synthesized using M-MLV RTase (Promega, USA). Next, mRNA expression was analyzed using SYBR Master Mixture (TAKARA, China) on an ABI Prism 7500 Real-Time System (Applied Biosystems, USA). β-Actin was used as an internal control. The relative expression of the target gene was normalized to β-actin expression using the $2^{-\Delta\Delta Ct}$ analysis method. The primer sequences were as follows: Sertad1 (5′-GCTGAGCAAAGGTCTGAAGC-3′ and 5′-GTGTTCACCACAAGCACCAG-3′) and β-actin (5′-AGCCATGTACGTAGCCATCC-3′ and 5′- CTCTCAGCTGTGGTGGTGAA-3′).

Western blot

After treatment, brain tissues and HT22 cells were collected and lysed using RIPA lysis buffer (Beyotime). The protein concentrations were then determined by the BCA protein assay kit (Beyotime). The proteins were separated by 10% SDS-PAGE and transferred onto PVDF membranes. The PVDF membranes were blocked using 5% bovine serum albumin (BSA) for 1 h at room temperature and incubated with the following primary antibodies: rabbit anti-Sertad1 (1:1,000, ab154066; Abcam), rabbit anti-CDK4 (1:2,000, 11026-1-AP; Proteintech), rabbit anti-p-Rb (S795) (1:500, ab131347; Abcam), rabbit anti-Rb (1:2,000, ab181616; Abcam), rabbit anti-B-Myb (1:500, 18896-1-AP; Proteintech), rabbit anti-Bim (1:500, 22037-1-AP; Proteintech), rabbit anti-Caspase3 (1:1,000, 19677-1-AP; Proteintech), and rabbit anti-β-actin (1:2,000, 20536-1-AP; Proteintech). The PVDF membranes were incubated overnight at 4°C and washed three times with TBST and incubated with a horseradish peroxidase conjugated goat anti-rabbit secondary antibody for 45 min at room temperature. Finally, the corresponding band was revealed using enhanced chemiluminescence reagents (Pierce Biotechnology).

Co-immunoprecipitation (Co-IP)

Co-IP was performed as described previously (Ding et al., 2018; Nguyen and Irby, 2017). Briefly, HT22 cells were transfected with pcDNA3.1 or Sertad1 ov plasmid for 48 h, and collected and lysed using cold RIPA lysis buffer (Beyotime) at 4°C for 30 min. The lysates were centrifuged at 14,000 × *g* for 15 min, and pre-cleared using protein A agarose at 4°C for 30 min. The protein A agarose was discarded by centrifugation at 1,000 × *g* for 5 min. Protein concentrations were then determined using the BCA protein assay kit (Beyotime). Specifically, the protein (50 μg) was incubated with anti-flag tag antibody or anti-CDK4 antibody at 4°C overnight. Next, protein A agarose was added to the antigen-antibody complex and incubated at 4°C for 2 h. The samples were washed five times using PBS and centrifuged at 1,000 × *g* for 5 min. The supernatant was discarded after each wash. Finally, the samples were resuspended by adding 25 μl of 1 × SDS-PAGE loading buffer, boiled for 5 min, and centrifuged

14,000 × *g* for 5 s. The supernatant (20 μl per lane) was examined by 10% SDS-PAGE and transferred onto PVDF membranes, which were blocked using 5% BSA for 1 h at room temperature and incubated with the following primary antibodies: rabbit anti-Sertad1 (1:1,000, ab154066; Abcam), rabbit anti-CDK4 (1:2,000, 11026-1-AP; Proteintech), rabbit anti-β-actin (1: 2,000, 20536-1-AP; Proteintech), and rabbit anti-flag tag (1:1,000, 80010-1-RR; Proteintech). The PVDF membranes were incubated overnight at 4°C and washed three times with TBST and incubated with the horseradish peroxidase conjugated goat anti-rabbit secondary antibody for 45 min at room temperature. Finally, the corresponding band was revealed using enhanced chemiluminescence reagents (Pierce Biotechnology).

Statistical analysis

Statistical analysis was performed using IBM SPSS Statistics (ver. 19; IBM, USA). The data are shown as the means ± SD. An unpaired Student's *t*-test was used for comparisons between two groups, and the differences among multiple groups were determined by ANOVA with Tukey's post-test. $P < 0.05$ was considered statistically significant.

RESULTS

Sertad1 expression was elevated in the MCAO model

To determine the role of Sertad1 during ischemic stroke, we first established the MCAO/R model in mice and examined the Sertad1 expression using RT-qPCR and Western blot. As shown in Figs. 1A and 1B, the Sertad1 mRNA and protein levels were significantly higher in the MCAO group than those in the sham group and peaked at 48 h after MCAO/R. We then determined the type of cell responsible for the increased Sertad1 after ischemic stroke. Forty-eight hours after MCAO/R, double-label immunohistochemistry was performed to analyze the localization of the immunofluorescence signals for Sertad1 with the neuronal marker NeuN, astrocytic marker GFAP and microglial marker Iba1 in the peri-infarct region of cortex and hippocampus. Our results showed that Sertad1 was mainly localized in neurons and upregulated only in neurons, not in astrocytes and microglia (Fig. 1C, Supplementary Fig. S1). These data suggested that Sertad1 may play a critical role in neurons during ischemic injury.

Downregulation of MCAO/R-induced Sertad1 by AAV-shSertad1

To determine the gene transduction efficiency of AAV, the EGFP signal of AAV was observed at 20 days and 40 days after AAV injection (AAV9-Syn-GFP-U6-negative control). As shown in Supplementary Fig. S2, the EGFP signal at 40 days after AAV infection was higher than that at 20 days after AAV infection. Thus, we established the MCAO/R model at 40 days after AAV infection. Forty-eight hours after MCAO/R, double-label immunohistochemistry was performed to analyze the localization of the immunofluorescence signals for Sertad1 (red) with the neuronal marker NeuN (blue). As shown in Fig. 2A, AAV-shSertad1 significantly inhibited the expression of Sertad1 in the peri-infarct region of the cortex and hippocampus compared with the AAV-shCon group. RT-qPCR and Western blot were used to confirm the *in vivo* knockdown efficiency of AAV infection. As shown in Figs. 2B and 2C, the mRNA and protein expression levels of Sertad1 in the peri-infarct region of cortex and hippocampus were significantly elevated than those in the sham group, whereas the expression of Sertad1 was significantly inhibited in the AAV-shSertad1 group than that in the AAV-shCon group.

Sertad1 inhibition ameliorated brain injury after MCAO/R

To determine the role of Sertad1 during the progression of ischemic stroke, a TTC analysis of brain sections was performed. Our results showed that the infarct volume at 48 h after MCAO/R was significantly increased, whereas the infarct volume in the AAV-shSertad1 group was significantly decreased compared with that in the AAV-shCon group (Fig. 3A). The neurological deficit score was used to evaluate neurological function after MCAO/R. As shown in Fig. 3B, MCAO markedly reduced neurological function, and neurological function in the AAV-shSertad1 group was significantly ameliorated compared with that in the AAV-shCon group. In addition, TUNEL staining was performed to detect the effect of Sertad1 on MCAO/R-induced neuronal death. As shown in Figs. 3C and 3D, neuronal death in the peri-infarct region of cortex and hippocampus at 48 h after MCAO/R was significantly elevated compared with that in the sham group, and Sertad1 inhibition by AAV-shSertad1 significantly decreased MCAO/R-induced neuronal death. In addition, Western blot was used to further confirm the role of Sertad1 in MCAO/R-induced neuronal apoptosis. As shown in Fig. 3E, the protein expression levels of Cleaved-caspase3 (a major factor in cell apoptosis) in the peri-infarct region of the cortex and hippocampus were significantly elevated than those in the sham group, and Cleaved-caspase3 protein expression was significantly inhibited in the AAV-shSertad1 group than that in the AAV-shCon group.

OGD/R induced neuronal injury and Sertad1 expression in HT22 cells

To determine the effects of OGD/R on neuronal injury, we established an OGD/R model in HT22 cells. As shown in Fig. 4A, cell viability was decreased in a time-dependent manner during OGD/R. Then, we verified the effects of OGD/R on Sertad1 expression. As shown in Figs. 4B and 4C, cells exposed to OGD/R exhibited increased Sertad1 mRNA and protein levels. The Sertad1 mRNA and protein levels peaked after 8 h of OGD and 24 h of reperfusion. On the basis of these results, we selected OGD for 8 h and reperfusion for 24 h in the subsequent cell experiments. HIF proteins are usually upregulated after cerebral ischemia and used to demonstrate OGD condition (Chavez and LaManna, 2002; Zhang et al., 2014). Thus, we detected HIF-1α protein expression in the HT22 cells after OGD for 8 h and reperfusion for 24 h. As shown in Supplementary Fig. S3, OGD/R significantly induced HIF-1α protein expression in HT22 cells. These results suggested the OGD model was successfully established. Additionally, TUNEL assay was used to confirm the effects of OGD/R on HT22 cells death. The results showed that OGD/R significantly induced cell death in the HT22 cells (Fig. 4D). Cleaved-caspase3 protein in the HT22 cells after OGD/R was

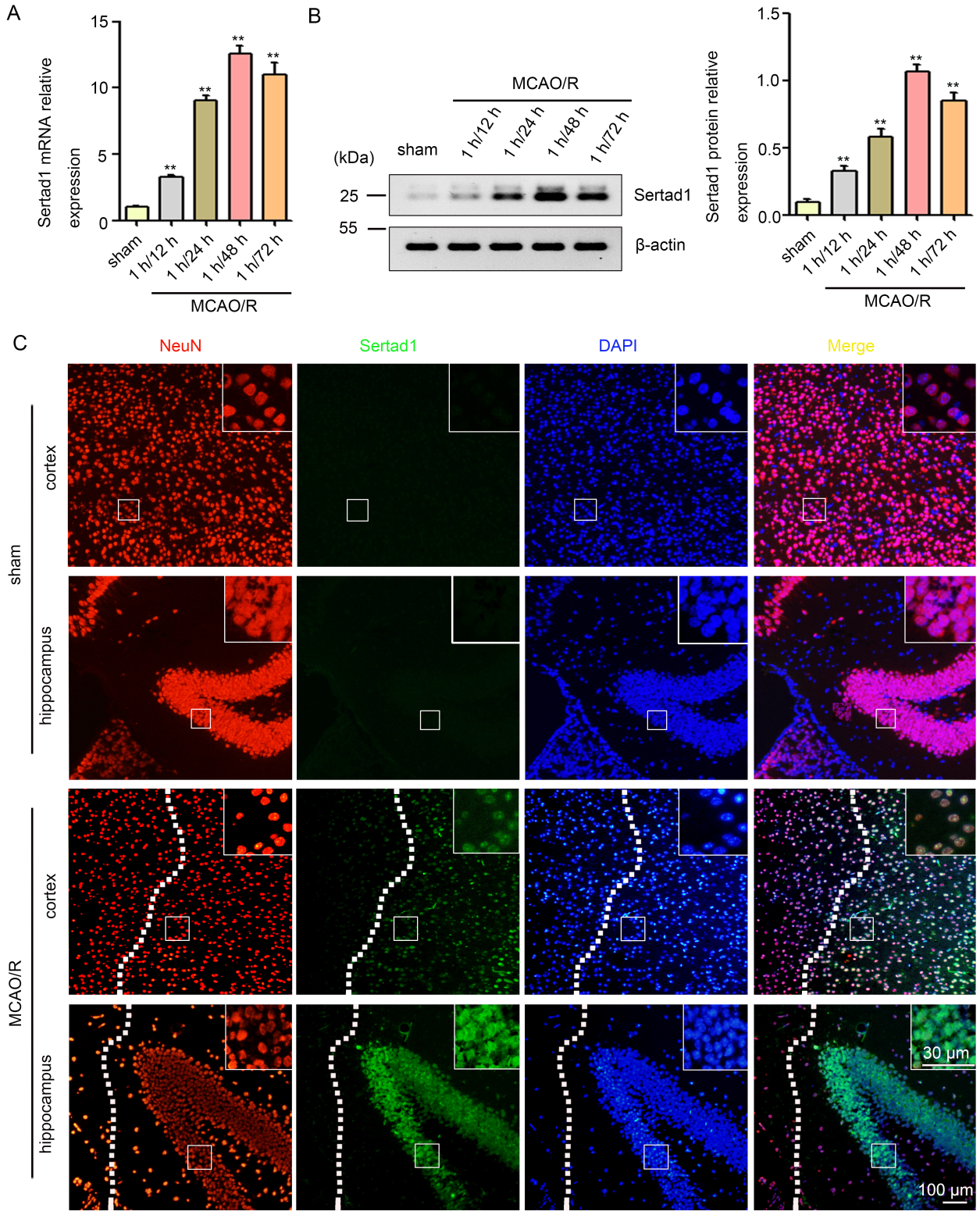

Fig. 1. Sertad1 is upregulated and mainly localized in neurons after MCAO/R. (A) The expression levels of Sertad1 mRNA were analyzed by RT-qPCR (n = 6). (B) The expression levels of Sertad1 protein were analyzed by Western blot (n = 6). (C) The immunofluorescence signal of Sertad1 (green) was colocalized with NeuN (neurons marker, red) in the peri-infarct region of the cortex and hippocampus after MCAO/R. Scale bars = 30 μm and 100 μm. $^{**}P < 0.01$ compared with the sham group.

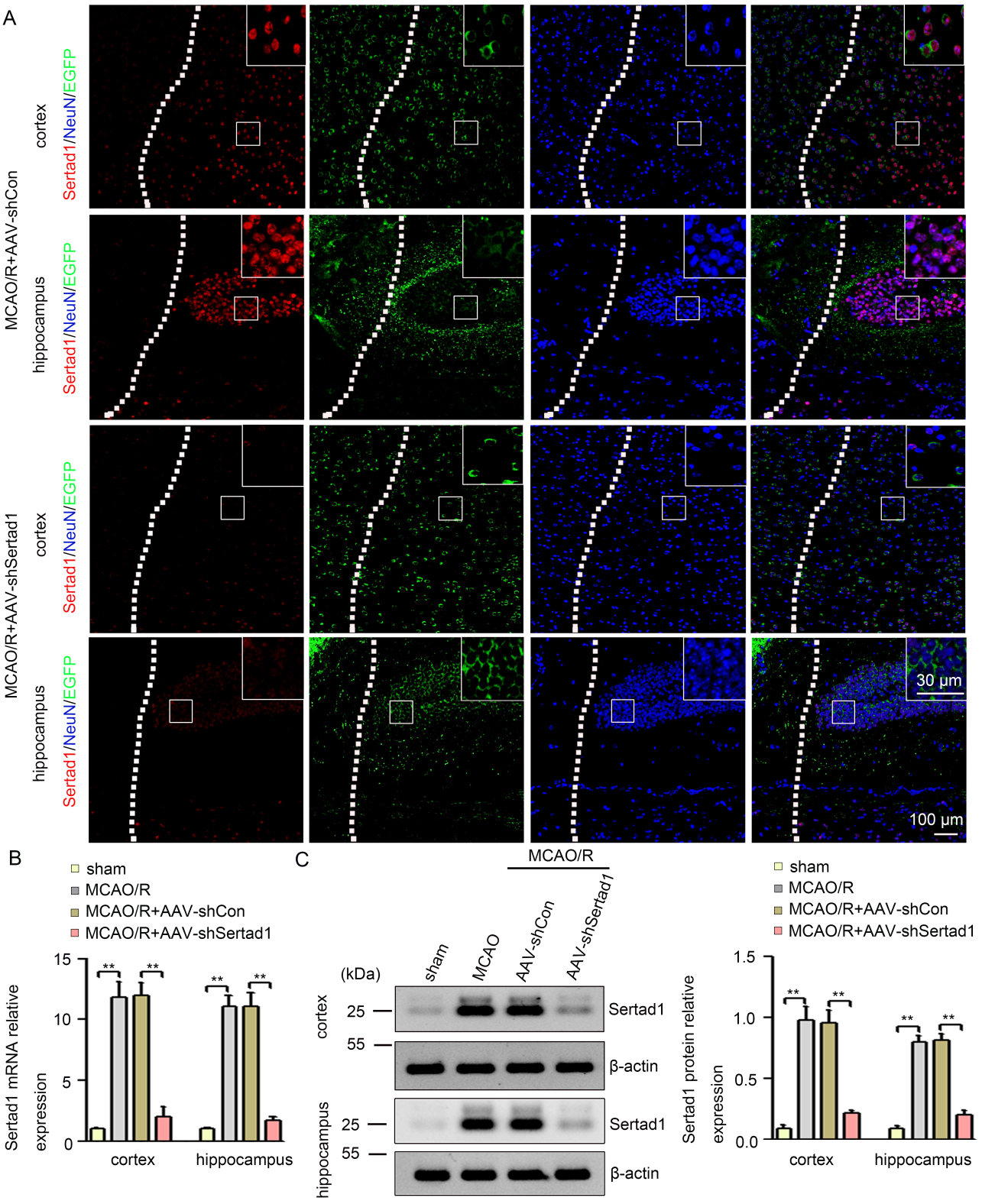

Fig. 2. Downregulation of MCAO/R-induced Sertad1 by AAV-shSertad1. (A) Immunofluorescence analysis was used to determine the silencing efficiency of AAV-shSertad1 in the peri-infarct region of the cortex and hippocampus 2 days after MCAO/R. Sections were stained for Sertad1 (red), NeuN (blue), and EGFP (green). Scale bars = 30 μm and 100 μm. (B and C) The silencing efficiency of AAV-shSertad1 2 days after MCAO/R was confirmed by RT-qPCR and Western blot (n = 6). $^{**}P < 0.01$.

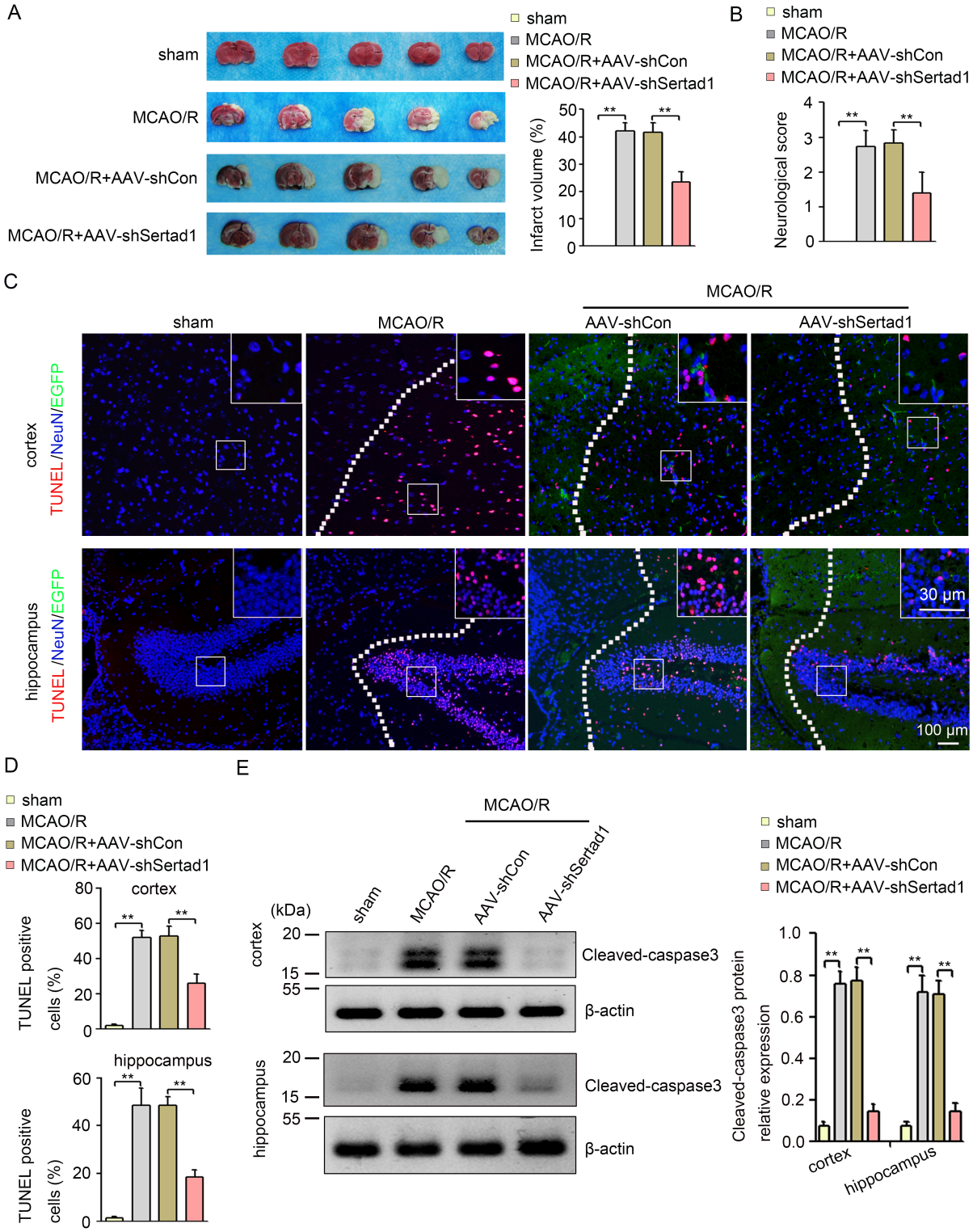

Fig. 3. Sertad1 inhibition ameliorated stroke outcomes. (A) TTC staining was used to determine the infarct volume in the mice that underwent the indicated treatment at 48 h after MCAO/R (n = 6). (B) Neurological function in the mice that underwent the indicated treatment was measured using the neurological deficit score at 48 h after MCAO/R (n = 18). (C and D) TUNEL assay was used to determine the dead neurons in the peri-infarct region of the cortex and hippocampus of mice at 48 h after MCAO/R. Sections were stained for TUNEL (red), NeuN (blue), and EGFP (green) (n = 6). Scale bars = 30 μm and 100 μm. (E) The expression levels of Cleaved-caspase3 protein in the peri-infarct region of the cortex and hippocampus of mice at 48 h after MCAO/R were analyzed using Western blot (n = 6). $^{**}P < 0.01$.

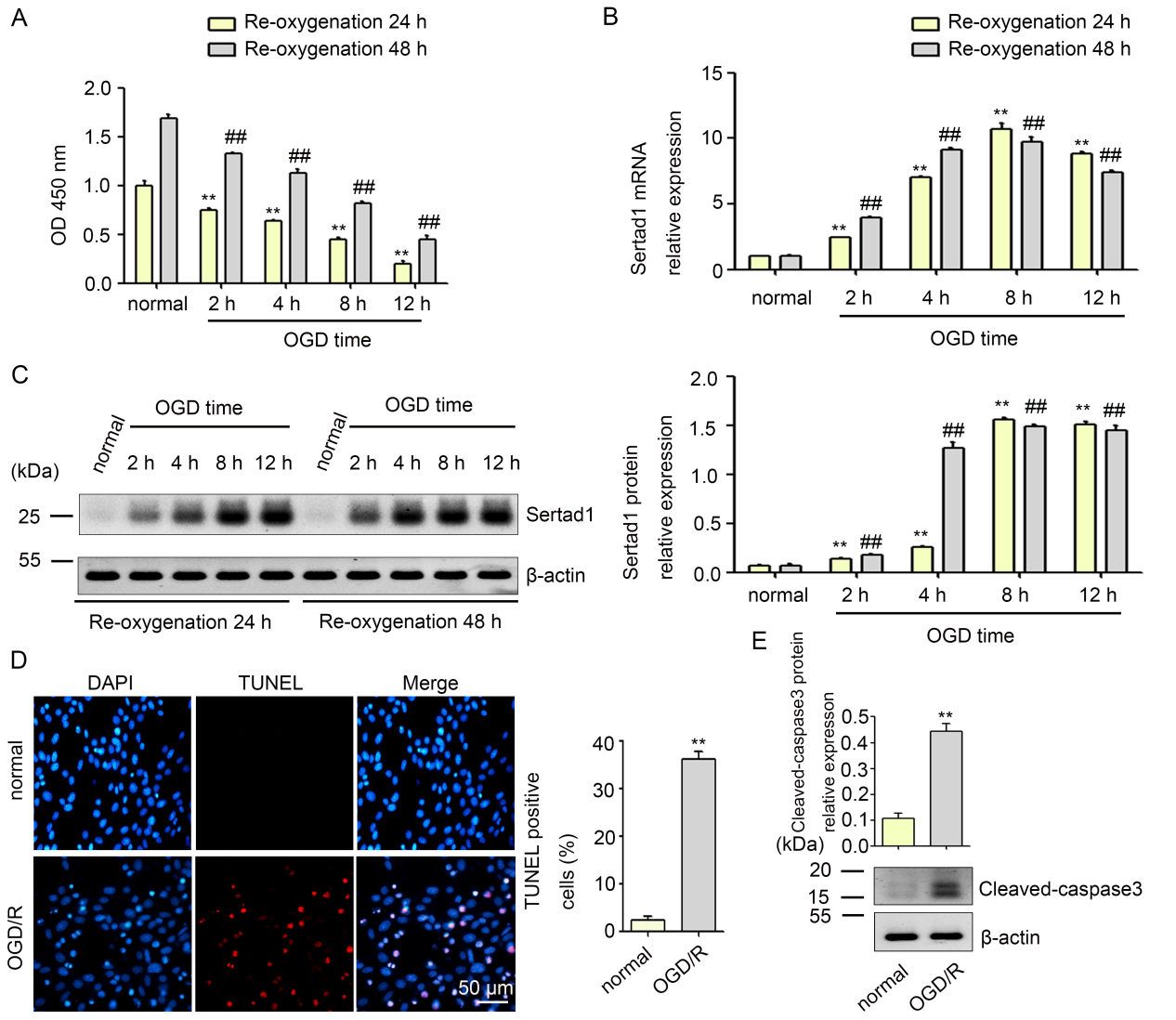

Fig. 4. Effect of OGD/R on cell viability, Sertad1 expression and apoptosis in HT22 cells. (A) HT22 cells were cultured in a glucose-free DMEM solution and maintained in a hypoxic chamber with 94% N_2, 1% O_2, and 5% CO_2 at 37°C for 2, 4, 8, or 12 h. Then, they were reoxygenated for 24 or 48 h in a complete medium. The HT22 cells in the normal group were subjected to OGD for 0 h and reoxygenated for 24 h or 48 h in a complete medium. Cell viability was determined using CCK-8. (B and C) The expression levels of Sertad1 mRNA and protein were analyzed using RT-qPCR and Western blot. (D) After OGD for 8 h and reperfusion for 24 h, the cell death of HT22 cells was measured by TUNEL. Scale bar = 50 μm. (E) The expression levels of Cleaved-caspase3 protein in HT22 cells after OGD/R were analyzed using Western blot. Data were presented as the mean ± SD obtained from three independent experiments for three well replicates. $^{**}P < 0.01$ compared with the normal group. $^{\#\#}P < 0.01$ compared with the normal group.

significantly increased compared with that in the normal group (Fig. 4E).

Upregulated Sertad1 was involved in neuronal injury induced by OGD/R in the HT22 cells

To verify the role of Sertad1 in OGD/R-induced neuronal injury, we synthesized Sertad1 siRNA and constructed Sertad1 overexpression plasmids. Western blot analysis showed that Sertad1 siRNA significantly decreased Sertad1 protein levels induced by OGD/R, whereas HT22 cells transfected with the Sertad1 overexpression plasmids exhibited higher Sertad1 protein levels than the pcDNA3.1 group (Fig. 5A). As shown in Fig. 5B, cell viability in the OGD/R group and OGD/R+si-Con groups was significantly lower than that in the normal group. Cell viability in the OGD/R+siSertad1 group was significantly higher than that in the OGD/R+siCon group (Fig. 5B). However, cell viability in the OGD/R+Sertad1 ov group was significantly lower than that in the OGD/R+pcDNA3.1 group (Fig. 5B). As shown in Figs. 5C and 5D, the OGD/R group and OGD/R+siCon groups had significantly higher percentages of TUNEL-positive cells than that in the normal group. The percentage of TUNEL-positive cells in the OGD/

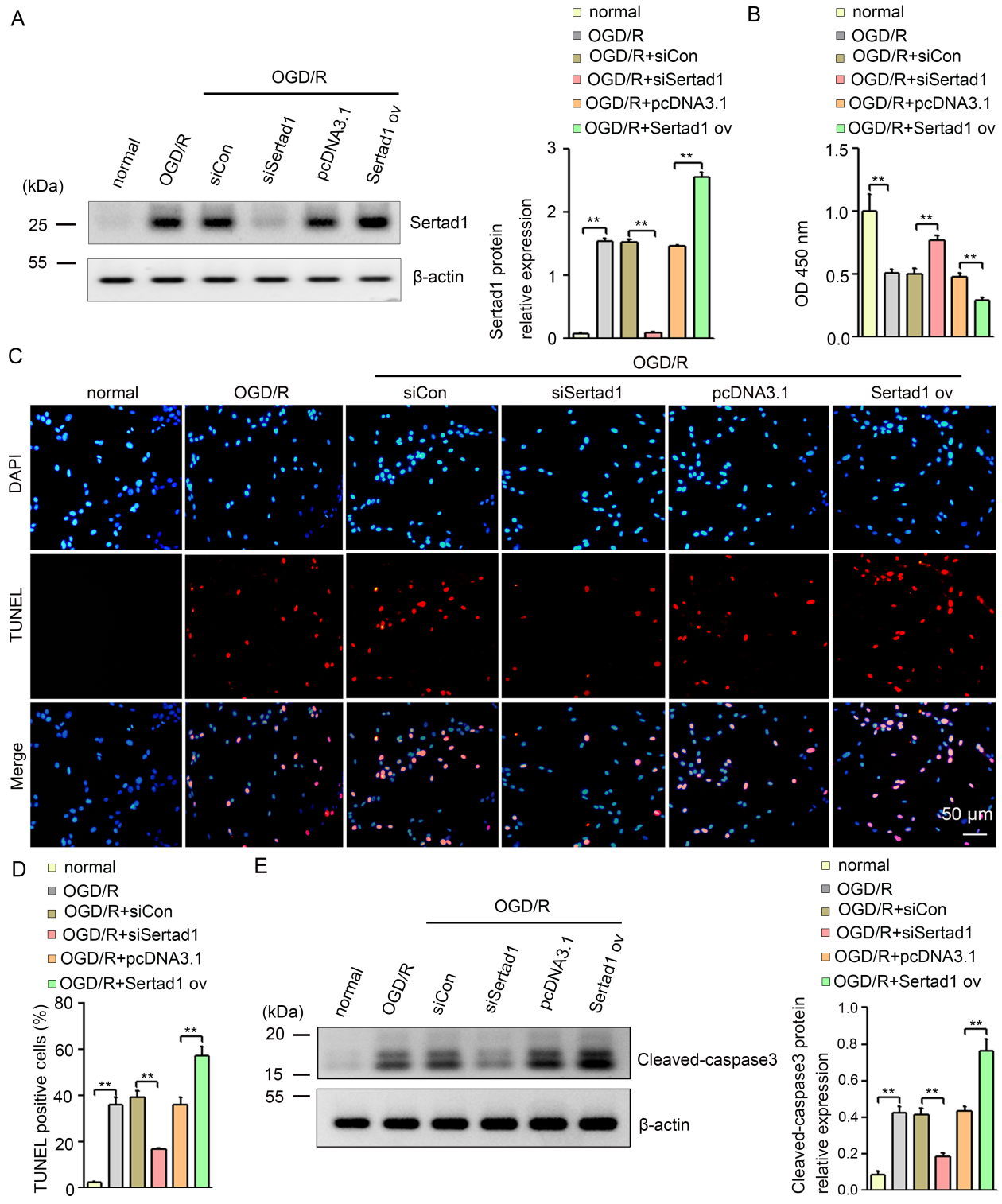

Fig. 5. OGD/R-induced Sertad1 upregulation was involved in neurological injury in HT22 cells. (A) HT22 cells were transfected with the scramble control siRNA (siCon), Sertad1 siRNA (siSertad1), pcDNA3.1 negative control plasmid (pcDNA3.1), or Sertad1-3flag expression plasmid (Sertad1 ov) for 48 h and then subjected to OGD for 8 h and reperfusion for 24 h. The expression levels of Sertad1 protein were analyzed by Western blot. (B) Cell viability was analyzed using CCK-8 assay. (C and D) Cell death was analyzed using TUNEL assay. (E) The expression levels of Cleaved-caspase3 protein were analyzed using Western blot. Data were presented as the mean ± SD obtained from three independent experiments. Scale bar = 50 μm. $^{**}P < 0.01$.

R+siSertad1 group was significantly lower than that in the OGD/R+siCon group (Figs. 5C and 5D). However, the percentage of TUNEL-positive cells in the OGD/R+Sertad1 ov group was significantly higher than that in the OGD/R+pcDNA3.1 group (Figs. 5C and 5D). Cleaved-caspase3 protein expression in the OGD/R group and OGD/R+siCon groups were significantly higher than that in the normal group (Fig. 5E), whereas Sertad1 inhibition significantly repressed OGD/R-induced Cleaved-caspase3 (Fig. 5E). In addition, Cleaved-caspase3 protein expression in the OGD/R+Sertad1 ov group was significantly higher than that in the OGD/R+pcDNA3.1 group (Fig. 5E).

Sertad1 regulated the CDK4/p-Rb pathway by directly binding CDK4 in HT22 cells during OGD/R

Sertad1 regulates the formation and activation of cyclin D/CDK4 complexes (Sugimoto et al., 1999). In addition, the activation of cyclin D/CDK4/pRb plays an important role in neuronal death induced by thrombin, DNA damage, NGF withdrawal or ischemic insult (Iyirhiaro et al., 2017; Liu and Greene, 2001; Rao et al., 2007; Rashidian et al., 2005). Thus, we aimed to determine whether Sertad1 can regulate the CDK4/p-Rb pathway in the HT22 cells during OGD/R. We performed Western blot to determine the effects of Sertad1 on the CDK4/p-Rb pathway. As shown in Fig. 6A, the expression levels of CDK4, p-Rb, B-Myb, and Bim proteins in the OGD/R group and OGD/R+siCon groups were significantly higher than those in the normal group. The expression levels of p-Rb, B-Myb, and Bim proteins in the OGD/R+siSertad1 group were significantly lower than those in the OGD/R+siCon group (Fig. 6A). However, the expression levels of p-Rb, B-Myb, and Bim proteins in the OGD/R+Sertad1 ov group were higher than those in the OGD/R+pcDNA3.1 group (Fig. 6A). Meanwhile, Sertad1 knockdown or overexpression did

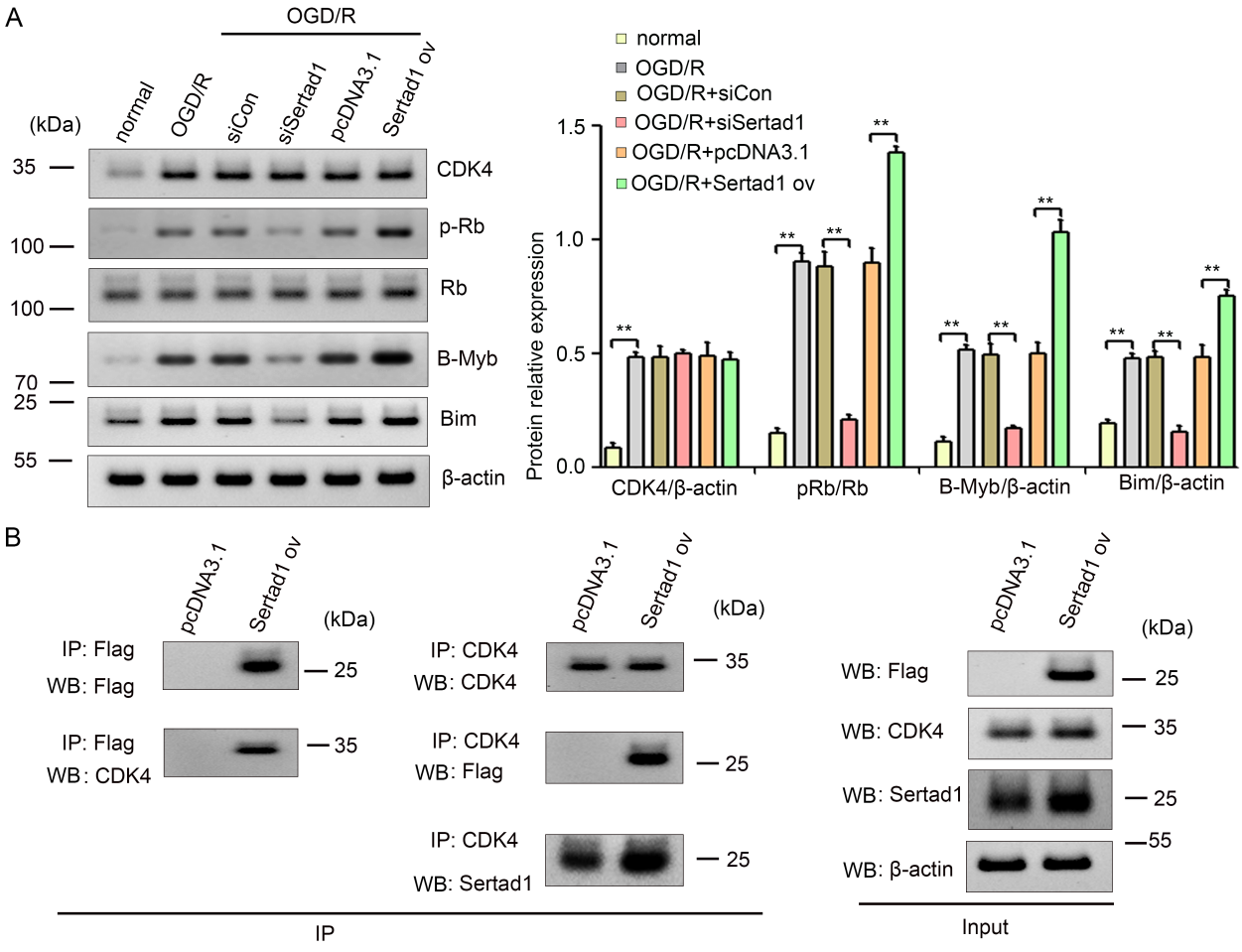

Fig. 6. Sertad1 promoted the CDK4/p-Rb pathway by directly binding CDK4 in HT22 cells during OGD/R. (A) HT22 cells were transfected with the scramble control siRNA (siCon), Sertad1 siRNA (siSertad1), pcDNA3.1 negative control plasmid (pcDNA3.1), or Sertad1-3flag expression plasmid (Sertad1 ov) for 48 h and then subjected to OGD for 8 h and reperfusion for 24 h. Western blot was used to determine the expression levels of CDK4, p-Rb, Rb, B-Myb, and Bim proteins. (B) HT22 cells were transfected with pcDNA3.1 negative control plasmid (pcDNA3.1) or Sertad1-3flag expression plasmid (Sertad1 ov). Whole cell lysates were precipitated with the indicated antibody. Whole cell lysates and precipitated proteins were analyzed by Western blot (WB) with the indicated antibodies. Data were presented as the mean ± SD obtained from three independent experiments. $**P < 0.01$.

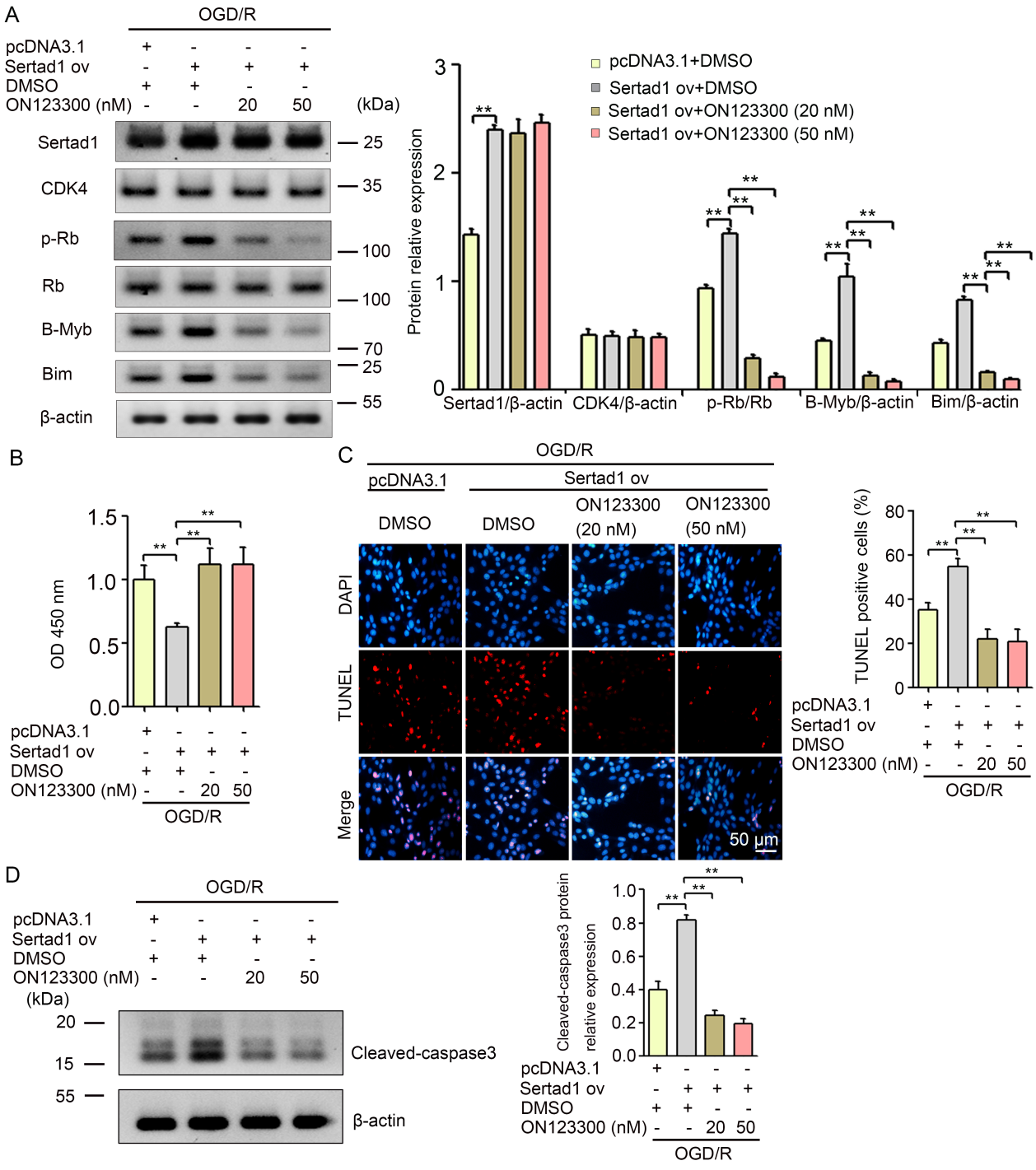

Fig. 7. Sertad1 contributed to OGD/R-induced neurological injury in the HT22 cells by regulating the CDK4/p-Rb pathway. (A) HT22 cells were transfected with the pcDNA3.1 negative control plasmid (pcDNA3.1) or Sertad1-3flag expression plasmid (Sertad1 ov). After 8 h, the medium was changed to fresh medium with DMSO, 20 nM ON123300, or 50 nM ON123300, and HT22 cells were further incubated for 48 h. HT22 cells were then subjected to OGD for 8 h and reperfusion for 24 h. Western blot was used to determine the expression levels of CDK4, p-Rb, Rb, B-Myb, and Bim proteins. (B and C) Cell viability and cell death was analyzed by CCK-8 and TUNEL assays, respectively. Scale bar = 50 μm. (D) The expression levels of Cleaved-caspase3 protein were analyzed using Western blot. Data were presented as the mean ± SD obtained from three independent experiments. $^{**}P < 0.01$.

not affect the CDK4 protein levels induced by OGD/R in the HT22 cells (Fig. 6A). To further determine whether Sertad1 can activate the CDK4/p-Rb pathway, Co-IP was performed using the anti-flag antibody and co-precipitated CDK4 was detected by an anti-CDK4 antibody. As shown in Fig. 6B, Sertad1 was found to be involved in the interaction with CDK4. Reciprocally, Co-IP was performed using the anti-CDK4 antibody and co-precipitated flag was detected by an anti-flag antibody or anti-Sertad1 antibody. The results showed that Sertad1 was involved in interactions with CDK4.

Sertad1 regulated OGD/R-induced neuronal injury in HT22 cells via the CDK4/p-Rb pathway

To determine whether Sertad1 can regulate OGD/R-induced neuronal injury via the CDK4/p-Rb pathway, we reversed the activation of the CDK4/p-Rb pathway in the HT22 cells

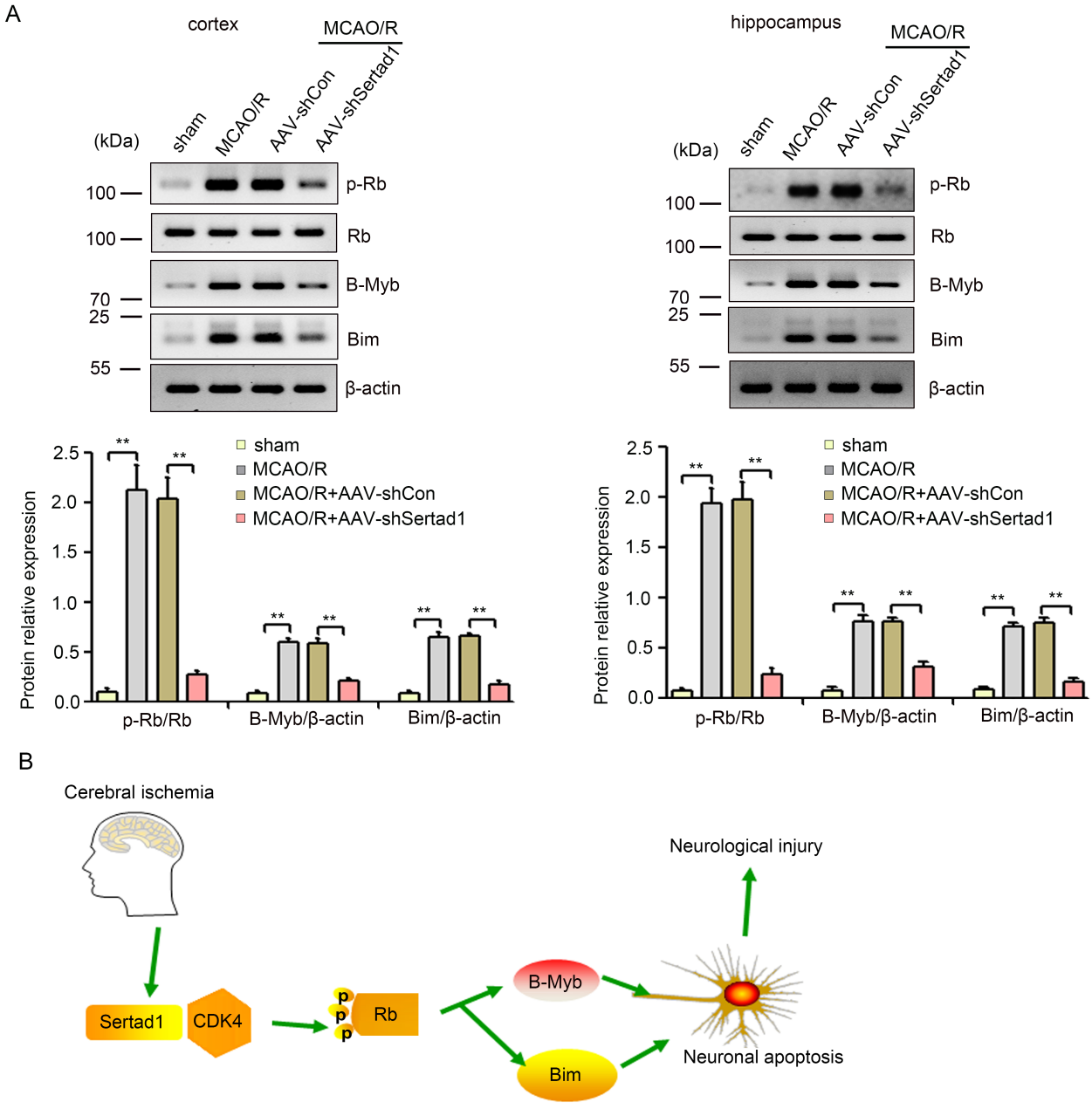

Fig. 8. Sertad1 regulated the CDK4/p-Rb pathway during stroke. (A) Western blot was used to determine the effects of Sertad1 on the expression levels of p-Rb, Rb, B-Myb, and Bim proteins in brain tissues from the peri-infarct region of the cortex and hippocampus 48 h after MCAO/R. (B) Schematic of the mechanism of Sertad1 in neuronal injury during stroke. Data were presented as the mean ± SD obtained from three independent experiments. $^{**}P < 0.01$.

using ON123300, which is a strong inhibitor of CDK4. Our results showed that the inhibition of the CDK4/p-Rb pathway reversed the increases in p-Rb, B-Myb, and Bim protein levels induced by Sertad1 overexpression during OGD/R (Fig. 7A). As shown in Fig. 7B, the cell viability in the Sertad1 ov+DMSO group was significantly lower than that in the pcDNA3.1+DMSO group, which was improved by ON123300 treatment at doses of 20 nM and 50 nM. The percentage of TUNEL-positive cells in the Sertad1 ov+DMSO group was significantly higher than that in the pcDNA3.1+DMSO group, in which the percentage decreased after ON123300 treatment with doses of 20 nM and 50 nM (Fig. 7C). In addition, Cleaved-caspase3 protein expression in the Sertad1 ov+DMSO group was significantly higher than that in the pcDNA3.1+DMSO group, which was decreased by ON123300 treatment at doses of 20 nM and 50 nM (Fig. 7D).

Sertad1 regulated the CDK4/p-Rb pathway during stroke

To confirm whether Sertad1 can regulate the CDK4/p-Rb pathway *in vivo*, Western blot was used to determine the effects of Sertad1 on the CDK4/p-Rb pathway. As shown in Fig. 8A, p-Rb, B-Myb, and Bim protein levels in the MCAO/R and MCAO/R+AAV-shCon groups were significantly higher than those in the sham group, whereas the expression levels of the same proteins in the MCAO/R+AAV-shSertad1 group were significantly lower than those in the MCAO/R+AAV-shCon group. Sertad1 may control neuronal injury by regulating the CDK4/p-Rb pathway during stroke (Fig. 8B).

DISCUSSION

In the present study, we first provided evidence that Sertad1 was significantly upregulated in the mouse brain after MCAO/R, and elevated Sertad1 was mainly occurred in neurons (Fig. 1C, Supplementary Fig. S1). In addition, Sertad1 expression was increased in HT22 cells after OGD/R (Figs. 4B and 4C). Consistent with our findings, Biswas et al. (2010) found that Sertad1 is induced by NGF withdrawal and β-amyloid in neurons. Moreover, Sertad1 knockdown protects cortical neurons from NGF withdrawal and β-amyloid-evoked cell death and degeneration (Biswas et al., 2010). Thus, Sertad1 may be involved in neuronal injury after ischemic stroke. However, the role and mechanism of Sertad1 in ischemic/hypoxic neurological injury remain unclear.

To determine the role of Sertad1 in neuronal injury induced by ischemic stroke, we constructed shSertad1 AAV and inhibited Sertad1 expression by injecting it into the mice before MCAO/R. We found that Sertad1 inhibition significantly reduced infarct volume and significantly ameliorated neurological function (Figs. 3A and 3B). Increasing evidence supports that the neuronal death in cerebral ischemia causes the irreversible loss of brain function (Wei et al., 2016). Therefore, we speculated that Sertad1 upregulation in neurons may induce neuronal injury, which causes irreversible loss of brain function. As expected, our results showed that Sertad1 repression significantly ameliorated MCAO/R-induced neuronal apoptosis *in vivo* (Figs. 3C-3E). To confirm the role of Sertad1 in neurological injury *in vitro*, we inhibited Sertad1 expression by siRNA and upregulated Sertad1 expression by the overexpression plasmids in HT22 cells before OGD/R. As expected, our results showed that Sertad1 knockdown significantly ameliorated OGD/R-induced inhibition of cell viability and apoptotic cell death in the HT22 cells, whereas Sertad1 overexpression significantly exacerbated the OGD/R-induced inhibition of cell viability and apoptotic cell death in the HT22 cells (Fig. 5). However, in breast cancer cell lines, hypoxia induces Sertad1 and tSertad1 inhibition accelerated cell apoptosis (Li et al., 2016). In addition, Sertad1 induces the proliferation of prostate cancer cells, thereby promoting prostate cancer progression (Hu et al., 2019). These results suggested that Sertad1 functions as an oncoprotein in tumors. Therefore, Sertad1 may have diverse functions under different pathological conditions.

Evidence has shown that Sertad1 directly binds and activates CDK4 and regulates the formation of cyclin D/CDK4 complexes (Sugimoto et al., 1999). The activation of cell cycle proteins, particularly CDK4, regulates neuronal death under pathological conditions. For example, one study found that CDK4 expression was increased in CA1 neurons following status epilepticus (SE) and that flavopiridol, a CDK4 inhibitor, attenuated SE-induced neuronal death (Kim and Kang, 2018). In the ischemic-reperfused rat retina, CDK4 inhibitor significantly ameliorated neuronal cell death (Sakamoto et al., 2011). Interestingly, CDK4 mediates neuronal death in stroke by phosphorylating Rb (Iyirhiaro et al., 2017; Rashidian et al., 2005). Thus, we hypothesized that Sertad1 regulates neuronal injury by activating CDK4 in HT22 cells during OGD/R. Our results showed that neither Sertad1 knockdown nor overexpression affected CDK4 protein levels induced by OGD/R in HT22 cells (Fig. 6A). Similar to our results, Hu et al. (2019) showed that Sertad1 knockdown did not affect androgen receptor (AR) mRNA expression and protein levels, but it could regulate prostate cancer progression by binding AR. In addition, Sertad1 has been shown to promote cell growth by antagonizing the function of the CDK inhibitor $p16^{INK4a}$, thereby affecting the kinase activity of CDK4 (Li et al., 2005; Sugimoto et al., 1999). In the present study, Co-IP assay showed that Sertad1 is involved in interactions with CDK4 (Fig. 6B). Activated CDK4 induces the hyper-phosphorylation of Rb, which in turn causes it and its bound chromatin modifiers to dissociate from members of the E2F transcription factor family, thereby resulting in B- and C-Myb expression de-repression and elevation of their levels (Greene et al., 2007; Liu and Greene, 2001). Mybs induce Bim expression by binding to its promoter, which results in caspases activation and apoptosis (Greene et al., 2007; Putcha et al., 2001). In addition, Sertad1 knockdown significantly reversed the increase of p-Rb, B-Myb, and Bim protein levels, while Sertad1 overexpression led to higher expression levels of these proteins (Fig. 6A). Thus, Sertad1 was involved in regulating the activation of the CDK4/p-Rb pathway and was not dependent on the regulation of CDK4 expression. Moreover, our results showed that the inhibition of the CDK4/p-Rb pathway by ON123300 reversed the increases in p-Rb, B-Myb, and Bim protein levels, decrease in cell viability and increase in cell apoptosis induced by Sertad1 overexpression during OGD/R (Fig. 7). To determine whether Sertad1 can regulate the CDK4/p-Rb pathway *in vivo*, we determined the effects

of Sertad1 on the CDK4/p-Rb pathway during stroke. Our results showed that the p-Rb, B-Myb, and Bim protein levels were significantly increased after MCAO/R, but the MCAO/R-induced expression of the proteins were suppressed by Sertad1 inhibition (Fig. 8A). These results suggested that Sertad1 regulates neuronal injury by activating the CDK4/p-Rb pathway during ischemic stroke (Fig. 8B).

In conclusion, our results demonstrated that Sertad1 was increased during ischemic stroke. Upregulated Sertad1 was mainly observed in the neurons and contributed to neuronal injury by activating the CDK4/p-Rb pathway. Sertad1 may be a novel therapeutic target for treating neuronal injury in stroke.

Note: Supplementary information is available on the Molecules and Cells website (www.molcells.org).

ACKNOWLEDGMENTS

This study was supported by grants from the Science and Technology Program of Chengguan District, Lanzhou City (grant No. 2017SHFZ0035) and the training program of the Cuiying graduate tutor.

AUTHOR CONTRIBUTIONS

J.L. and H.Z. conceived and wrote the manuscript. J.L. performed the experiments. B.L., Y.B., J.G., and J.H. provided technical support. J.L., J.G., and Y.Z. analyzed the data. All authors participated in review of the manuscript.

CONFLICT OF INTEREST

The authors have no potential conflicts of interest to disclose.

ORCID

Jianxiong Li https://orcid.org/0000-0003-2649-3045
Bin Li https://orcid.org/0000-0001-8385-0833
Yujie Bu https://orcid.org/0000-0002-2087-6670
Hailin Zhang https://orcid.org/0000-0002-0827-1425
Jia Guo https://orcid.org/0000-0001-8408-785X
Jianping Hu https://orcid.org/0000-0003-2629-8653
Yanfang Zhang https://orcid.org/0000-0002-9652-2393

REFERENCES

Adams, H.P., Jr. (2001). Treatment of acute ischemic stroke: selecting the right treatment for the right patient. Eur. Neurol. *45*, 61-66.

Auriel, E. and Bornstein, N.M. (2010). Neuroprotection in acute ischemic stroke--current status. J. Cell. Mol. Med. *14*, 2200-2202.

Biswas, S.C., Zhang, Y., Iyirhiaro, G., Willett, R.T., Rodriguez Gonzalez, Y., Cregan, S.P., Slack, R.S., Park, D.S., and Greene, L.A. (2010). Sertad1 plays an essential role in developmental and pathological neuron death. J. Neurosci. *30*, 3973-3982.

Chavez, J.C. and LaManna, J.C. (2002). Activation of hypoxia-inducible factor-1 in the rat cerebral cortex after transient global ischemia: potential role of insulin-like growth factor-1. J. Neurosci. *22*, 8922-8931.

Chen, T., Liu, W., Chao, X., Qu, Y., Zhang, L., Luo, P., Xie, K., Huo, J., and Fei, Z. (2011). Neuroprotective effect of osthole against oxygen and glucose deprivation in rat cortical neurons: involvement of mitogen-activated protein kinase pathway. Neuroscience *183*, 203-211.

Ding, C., He, J., Zhao, J., Li, J., Chen, J., Liao, W., Zeng, Y., Zhong, J., Wei, C., Zhang, L., et al. (2018). β-catenin regulates IRF3-mediated innate immune signalling in colorectal cancer. Cell Prolif. *51*, e12464.

Greene, L.A., Liu, D.X., Troy, C.M., and Biswas, S.C. (2007). Cell cycle molecules define a pathway required for neuron death in development and disease. Biochim. Biophys. Acta *1772*, 392-401.

Hacke, W., Kaste, M., Bluhmki, E., Brozman, M., Dávalos, A., Guidetti, D., Larrue, V., Lees, K.R., Medeghri, Z., Machnig, T., et al. (2008). Thrombolysis with alteplase 3 to 4.5 hours after acute ischemic stroke. N. Engl. J. Med. *359*, 1317-1329.

Hu, B., Hu, H., Yin, M., Sun, Z., Chen, X., Li, Y., Sun, Z., Liu, C., Li, L., and Qiu, Y. (2019). Sertad1 promotes prostate cancer progression through binding androgen receptor ligand binding domain. Int. J. Cancer *144*, 558-568.

Iyirhiaro, G.O., Im, D.S., Boonying, W., Callaghan, S.M., During, M.J., Slack, R.S., and Park, D.S. (2017). Cdc25A is a critical mediator of ischemic neuronal death *in vitro* and *in vivo*. J. Neurosci. *37*, 6729-6740.

Jin, J., Sun, H., Liu, D., Wang, H., Liu, Q., Chen, H., Zhong, D., and Li, G. (2019). LRG1 promotes apoptosis and autophagy through the TGFβ-smad1/5 signaling pathway to exacerbate ischemia/reperfusion injury. Neuroscience *413*, 123-134.

Kim, J.E. and Kang, T.C. (2018). Suppression of nucleocytoplasmic $p27^{Kip1}$ export attenuates CDK4-mediated neuronal death induced by status epilepticus. Neurosci. Res. *132*, 46-52.

Kuo, P.C., Scofield, B.A., Yu, I.C., Chang, F.L., Ganea, D., and Yen, J.H. (2016). Interferon-β modulates inflammatory response in cerebral ischemia. J. Am. Heart Assoc. *5*, e002610.

Kuriakose, D. and Xiao, Z. (2020). Pathophysiology and treatment of stroke: present status and future perspectives. Int. J. Mol. Sci. *21*, 7609.

Lai, I.L., Wang, S.Y., Yao, Y.L., and Yang, W.M. (2007). Transcriptional and subcellular regulation of the TRIP-Br family. Gene *388*, 102-109.

Li, C., Jung, S., Yang, Y., Kim, K.I., Lim, J.S., Cheon, C.I., and Lee, M.S. (2016). Inhibitory role of TRIP-Br1 oncoprotein in hypoxia-induced apoptosis in breast cancer cell lines. Int. J. Oncol. *48*, 2639-2646.

Li, J., Muscarella, P., Joo, S.H., Knobloch, T.J., Melvin, W.S., Weghorst, C.M., and Tsai, M.D. (2005). Dissection of CDK4-binding and transactivation activities of p34(SEI-1) and comparison between functions of p34(SEI-1) and p16(INK4A). Biochemistry *44*, 13246-13256.

Liu, D.X. and Greene, L.A. (2001). Regulation of neuronal survival and death by E2F-dependent gene repression and derepression. Neuron *32*, 425-438.

Liu, M., Xu, Z., Wang, L., Zhang, L., Liu, Y., Cao, J., Fu, Q., Liu, Y., Li, H., Lou, J., et al. (2020). Cottonseed oil alleviates ischemic stroke injury by inhibiting the inflammatory activation of microglia and astrocyte. J. Neuroinflammation *17*, 270.

Liu, S.B., Zhang, N., Guo, Y.Y., Zhao, R., Shi, T.Y., Feng, S.F., Wang, S.Q., Yang, Q., Li, X.Q., Wu, Y.M., et al. (2012). G-protein-coupled receptor 30 mediates rapid neuroprotective effects of estrogen via depression of NR2B-containing NMDA receptors. J. Neurosci. *32*, 4887-4900.

Longa, E.Z., Weinstein, P.R., Carlson, S., and Cummins, R. (1989). Reversible middle cerebral artery occlusion without craniectomy in rats. Stroke *20*, 84-91.

Nguyen, J.Q. and Irby, R.B. (2017). TRIM21 is a novel regulator of Par-4 in colon and pancreatic cancer cells. Cancer Biol. Ther. *18*, 16-25.

Putcha, G.V., Moulder, K.L., Golden, J.P., Bouillet, P., Adams, J.A., Strasser, A., and Johnson, E.M. (2001). Induction of BIM, a proapoptotic BH3-only BCL-2 family member, is critical for neuronal apoptosis. Neuron *29,* 615-628.

Rao, H.V., Thirumangalakudi, L., Desmond, P., and Grammas, P. (2007). Cyclin D1, cdk4, and Bim are involved in thrombin-induced apoptosis in cultured cortical neurons. J. Neurochem. *101*, 498-505.

Rashidian, J., Iyirhiaro, G., Aleyasin, H., Rios, M., Vincent, I., Callaghan, S., Bland, RJ., Slack, R.S., During, M.J., and Park, D.S. (2005). Multiple cyclin-dependent kinases signals are critical mediators of ischemia/hypoxic

neuronal death in vitro and in vivo. Proc. Natl. Acad. Sci. U. S. A. *102*, 14080-14085.

Russo, T., Felzani, G., and Marini, C. (2011). Stroke in the very old: a systematic review of studies on incidence, outcome, and resource use. J. Aging Res. *2011*, 108785.

Sakamoto, K., Ohki, K., Saitov, M., Nakahara, T., and Ishii, K. (2011). Small molecule cyclin-dependent kinase inhibitors protect against neuronal cell death in the ischemic-reperfused rat retina. J. Ocul. Pharmacol. Ther. *27*, 419-425.

Sugimoto, M., Nakamura, T., Ohtani, N., Hampson, L., Hampson, I.N., Shimamoto, A., Furuichi, Y., Okumura, K., Niwa, S., Taya, Y., et al. (1999). Regulation of CDK4 activity by a novel CDK4-binding protein, p34(SEI-1). Genes Dev. *13*, 3027-3033.

Wang, L., Lu, Y., Guan, H., Jiang, D., Guan, Y., Zhang, X., Nakano, H., Zhou, Y., Zhang, Y., Yang, L., et al. (2013). Tumor necrosis factor receptor-associated factor 5 is an essential mediator of ischemic brain infarction. J. Neurochem. *126*, 400-414.

Wei, N., Xiao, L., Xue, R., Zhang, D., Zhou, J., Ren, H., Guo, S., and Xu, J. (2016). MicroRNA-9 mediates the cell apoptosis by targeting Bcl2l11 in ischemic stroke. Mol. Neurobiol. *53*, 6809-6817.

Wu, R., Li, X., Xu, P., Huang, L., Cheng, J., Huang, X., Jiang, J., Wu, L.J., and Tang, Y. (2017). TREM2 protects against cerebral ischemia/reperfusion injury. Mol. Brain *10*, 20.

Xu, H., Qin, W., Hu, X., Mu, S., Zhu, J., Lu, W., and Luo, Y. (2018). Lentivirus-mediated overexpression of OTULIN ameliorates microglia activation and neuroinflammation by depressing the activation of the NF-κB signaling pathway in cerebral ischemia/reperfusion rats. J. Neuroinflammation *15*, 83.

You, J., Liu, J., Bao, Y., Wang, L., Yu, Y., Wang, L., Wu, D., Liu, C., Wang, N., Wang, F., et al. (2017). SEI1 induces genomic instability by inhibiting DNA damage response in ovarian cancer. Cancer Lett. *385*, 271-279.

Zhang, Z., Qin, P., Deng, Y., Ma, Z., Guo, H., Guo, H., Hou, Y., Wang, S., Zou, W., Sun, Y., et al. (2018). The novel estrogenic receptor GPR30 alleviates ischemic injury by inhibiting TLR4-mediated microglial inflammation. J. Neuroinflammation *15*, 206.

Zhang, Z., Yan, J., Taheri, S., Liu, K.J., and Shi, H. (2014). Hypoxia-inducible factor 1 contributes to N-acetylcysteine's protection in stroke. Free Radic. Biol. Med. *68*, 8-21.